Self-Assembled InAsP and InAlAs Nanowires on Graphene via Pseudo-van der Waals Epitaxy

Mohadeseh A. Baboli[1,2], Michael A. Slocum[2], Alessandro Giussani[2], and Seth M. Hubbard[1,2], Parsian K. Mohseni[1,2]
[1]Microsystems Engineering, Rochester Institute of Technology, Rochester, NY, United States, email: pkmohseni@rit.edu
[2]NanoPower Research Laboratory, Rochester Institute of Technology, Rochester, NY, United States

***Abstract*—**Vertically-aligned, high aspect ratio $InAs_yP_{1-y}$, $In_xAl_{1-x}As$, and core-shell InAsP-InP nanowires (NWs) are grown directly on two-dimensional (2-D) monolayer graphene via seed-free pseudo-van der Waals epitaxy (vdWE), as reported here for the first time. Growth is achieved using metalorganic chemical vapor deposition (MOCVD). By altering growth temperature and molar flow ratio of precursors, the composition of $InAs_yP_{1-y}$ NWs can be tuned within the $1 \leq y \leq 0.8$ range. Similarly, by tuning the group-III precursor flow rates, $In_xAl_{1-x}As$ composition can be modified in the $1 \leq x \leq 0.5$ range. NW morphology and NW array number density variances are measured for different ternary compositions as functions of precursor flow rates and growth temperature.

I. Introduction

Functional 2-D materials, such as graphene, have shown promising performance in many applications such as nanoelectronics [1] and photovoltaics [2]. Monolithic integration of III-V semiconductors with graphene and other 2-D nanosheets can be realized via growth of high aspect ratio NW structures. Such heteroepitaxial growth may proceed without sacrificing crystalline quality, due to an absence of strain sharing between substrate and epilayer [3, 4]. In recent years, nano-hybrid materials systems consisting of GaAs, InAs, InGaAs, and InAsSb NWs on graphene have been demonstrated through the vdWE approach [3, 4, 5]. In this growth mode, weak vdW forces, which are formed between a 2-D nanomaterial with no available surface dangling bonds and the III-V epilayer, can accommodate dislocation-free crystalline NW formation. Here, the 2-D nanosheet offers limited possibilities for arrangement of the overlaying III-V lattice. For the specific case of graphene, there are three available adsorption sites on the hexagonal carbon rings of graphene: (1) above a hollow site at the center of C-rings (H-site), (2) on top of a carbon atom (T-site), and (3) above the bridge of two neighboring carbon atoms (B-site) [6]. Based on the lattice constant of different III-V compounds and the finite number of atomic arrangements on graphene, Munshi et al. proposed a model that describes atomic configurations at the growth interface during vdWE [6]. Additionally, from a thermodynamic perspective, the binding energy between a specific adatom and underlying carbon atoms is unique for each H-, T-, and B-sites [7, 8]. Thus, for any specific growth species, only one of the three sites is energetically favorable.

Growth of III-V NWs on graphene has been realized through various mechanisms, such as self-catalyzed or Au-assisted vapor-liquid-solid (VLS) growth using molecular beam epitaxy (MBE) and MOCVD [6, 9]. Additionally, vertically oriented InAs and InGaAs can also be formed on inert graphitic surfaces through a self-assembly mechanism, which unlike other methods requires no pre-growth lithography step or deposition of metallic seeding agents [3, 4, 10]. However, to our knowledge, no studies have been reported on seed-free heterogeneous integration of InAsP and InAlAs NW arrays on single layer graphene (SLG) via the vdWE approach. Here, we present compositional and morphological tuning of hybrid ternary III-V-on-2-D nanomaterials systems enabled by NW self-assembly using MOCVD. Variations in NW morphology and number density are considered with respect to compositionally-dependent atomic configuration and adatom binding energy factors.

II. Experimental Details

Growth of NWs on SLG nanosheets was performed in an Aixtron 3×2" close coupled showerhead MOCVD reactor. Trimethyl-indium [TMIn, $(CH_3)_3In$] and trimethyl-aluminum [TMAl, $(CH_3)_6Al_2$] were used as group-III precursors; arsine (AsH_3) and phosphine (PH_3) were used for supply of group-V growth species.

In the present work, $InAs_yP_{1-y}$ NWs were grown using various hydride precursor molar flow ratios, defined by $\rho_{PH_3} = \frac{\chi_{PH_3}}{\chi_{PH_3} + \chi_{AsH_3}}$, where χ_{PH_3} and χ_{AsH_3} represent the molar flow rate of AsH_3 and PH_3, respectively. Similarly, $In_xAl_{1-x}As$ NW compositions were modified by varying the molar flow ratio of metalorganic precursors, defined by $\rho_{TMAl} = \frac{\chi_{TMAl}}{\chi_{TMIn} + \chi_{TMAl}}$, where χ_{TMIn} and χ_{TMAl} represent the molar flow rate of TMIn and TMAl, respectively. Growth temperatures (T_G) in the 600 °C to 750 °C range were investigated. In all cases, samples were heated to the desired growth temperature under a constant AsH_3 flow prior to growth initiation. The onset of crystal growth was marked by the introduction of group-III precursor(s). After a growth duration of 300 s, samples where cooled under constant supply of group-V precursors. For all samples, hydrogen (H_2) was used as the carrier gas with total flow of 7 L/min, and the reactor pressure was maintained at 100 mBar.

Samples were imaged with Hitachi S-4000 and TESCAN MIRA 3 scanning electron microscopes (SEM). X-ray diffraction (XRD) measurements were made using a Bruker D8 high-resolution X-ray diffractometer.

III. Results and Discussions

The focus of this study is to investigate self-assembly of InAsP and InAlAs NWs on SLG through the vdWE approach, and to explore the influence of key growth parameters on the

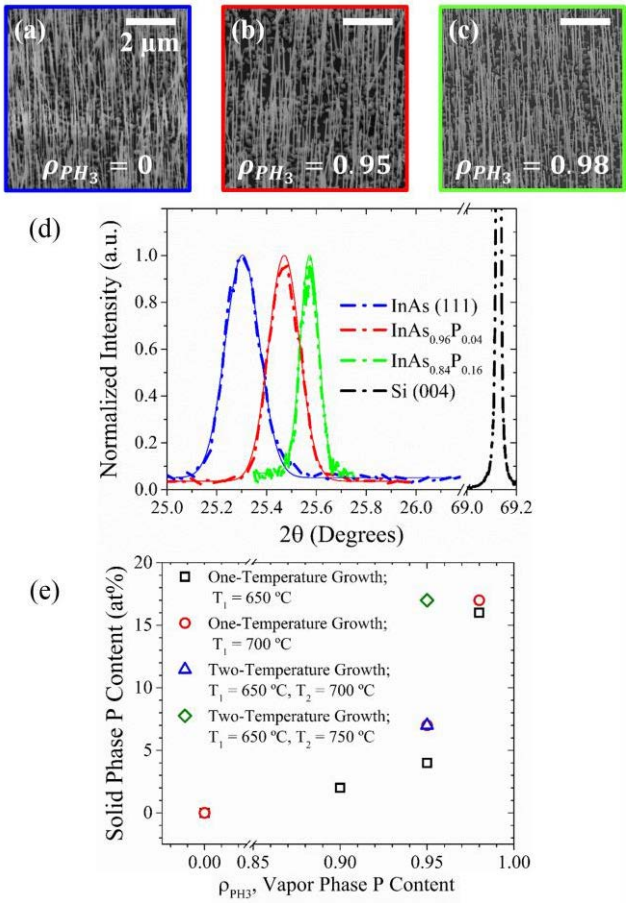

Fig. 1. 45°-tilted SEM image of $InAs_yP_{1-y}$ NWs grown at T_G = 650 °C for ρ_{PH_3} of (a) 0, (b) 0.95, (c) 0.98. All scale bars indicate 2 µm. (d) XRD specular 2θ-ω scans used to quantify the InAsP solid phase P-content. (e) Summary of solid phase P-content as a function of ρ_{PH_3} for all one- and two-temperature InAsP growths.

composition and morphology of resulting NWs. Growth of these two ternary III-V compounds is then compared with the well-studied case of binary InAs NWs on SLG. Firstly, vertically oriented ternary $InAs_yP_{1-y}$ NWs (i.e., for $1 \leq y \leq 0.8$) were grown on SLG through vdWE. Three sets of experiments were carried out to study the incorporation of solid phase phosphorous in InAsP NWs. In the first experiment, T_G was set to 650 °C while ρ_{PH_3} was varied from 0 to 0.98. In Fig. 1(a), InAs NWs (ρ_{PH_3} = 0) are compared to InAsP NWs grown under (b) ρ_{PH_3} = 0.95 and (c) ρ_{PH_3} = 0.98. Since nucleation sites are not limited to any patterned openings or catalyst seeds, self-assembly by vdWE results in growth of NWs as well as parasitic islands. NW lengths, diameters and number density, as well as areal density of parasitic islands are independent of ρ_{PH_3}. Fig. 1(d) shows XRD measurements from as-grown InAsP NWs used to quantify solid phase phosphorous content for ρ_{PH_3} = 0.95 (red plot) and ρ_{PH_3} = 0.98 (green plot). Compositional analysis of this sample set indicates P-incorporation increases from 4 at% to 16 at% by increasing ρ_{PH_3} from 0.95 to 0.98.

This experiment was also repeated at T_G = 700 °C for the same molar flow ratios. As before, NW morphology and number density, as well as parasitic island coverage were

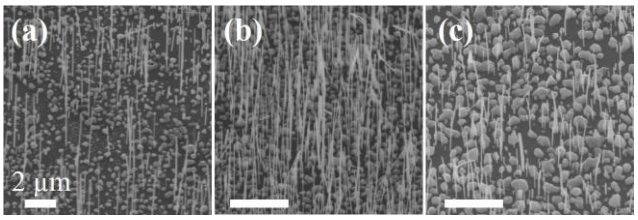

Fig. 2. (a) One-temperature InAsP NWs at T_G = 700 °C. InAs-$InAs_yP_{1-y}$ NWs grown under two-temperature regimes: (b) T_{G1} = 650 °C, T_{G2} = 700 °C, (c) T_{G1} = 650 °C, T_{G2} = 750 °C. All InAsP segments formed under ρ_{PH_3} = 0.95. All scale bars indicate 2 µm.

observed to be independent of ρ_{PH_3}. Increasing ρ_{PH_3} from 0.95 to 0.98 resulted in a composition change from $InAs_{0.93}P_{0.07}$ to $InAs_{0.84}P_{0.16}$. Increased solid phase P-content is likely due to higher PH_3 decomposition efficiency at elevated T_G [11].

However, increasing T_G adversely affects the NW number density. The same trend was also observed for case of InAs NWs on graphene [3]. To overcome this challenge, two-temperature growths were performed in a third-experiment. InAs growth was first initiated at a low T_G of 650 °C for 60 s to establish a high NW number density. Then T_G was ramped up to 700 °C and 750 °C, in different runs, while ρ_{PH_3} was raised to 0.95 in order to incorporate a higher P-content in the solid phase over a period of 240 s. Fig 1(e) summarizes results of XRD measurements for all three experiments, where solid phase phosphorus content is plotted as a function of ρ_{PH_3}. A direct comparison between growths of InAsP NWs under the above set of conditions indicates a non-linear P-incorporation trend for different growth temperatures, which is in agreement with bulk InAsP growth trends by MOCVD [11].

Fig. 2(a) shows $InAs_{0.93}P_{0.07}$ NWs grown with ρ_{PH_3} = 0.95 at T_G = 700 °C in a one-temperature regime, where a low NW number density is observed. However, Fig. 2b shows that by using a two-temperature growth sequence (i.e., T_{G1} = 650 °C; T_{G2} = 700 °C at ρ_{PH_3} = 0.95), a high density array of InAsP NWs with the same P-content (i.e., 7 at%) can be achieved. As expected, increasing T_{G2} to 750 °C results in NW number density reduction, but enables P-content enhancement for growth of $InAs_{0.83}P_{0.17}$ NWs. Similar temperature-dependent density trends were observed for InAs NWs on SLG [3]. Importantly, XRD measurements show no evidence of compositional phase segregation for InAsP NWs investigated here, which is in contrast to the case of InGaAs NWs on SLG where the ternary phase is formed by group-III alloying [4].

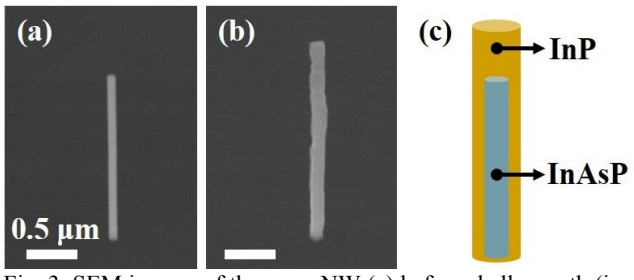

Fig. 3. SEM images of the same NW (a) before shell growth (i.e., only InAsP core segment) and (b) after InP shell growth (i.e. core-shell structure). (c) Schematic of core-shell InAsP-InP NW. All scale bars indicate 0.5 µm.

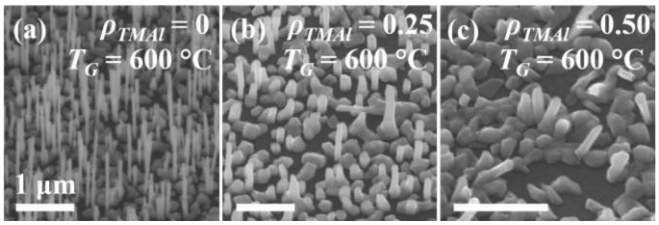

Fig. 4. 45º tilted-view SEM images of as-grown $In_xAl_{1-x}As$ NWs on SLG at (a) ρ_{TMAl} of 0, (b) ρ_{TMAl} of 0.25, and (c) ρ_{TMAl} of 0.50. All scale bars represent 1 µm.

Our results indicate that vdWE of high P-content $InAs_yP_{1-y}$ for $y < 0.8$ on SLG is difficult to achieve via direct self-assembly within the explored growth parameter space. However, higher P-content InAsP and even binary InP shell segments can be formed on existing InAsP NW core segments grown on SLG, as shown in Fig. 3.

In a separate study, vdWE of $In_xAl_{1-x}As$ NWs on SLG was explored in two sets of experiments. Firstly, at constant T_G = 600 °C, $In_xAl_{1-x}As$ NWs are grown with ρ_{TMAl} between 0 and 0.50 at a constant V/III ratio of 25. Fig. 4 shows 45° tilted-view SEM images of InAlAs grown on SLG, at (a) ρ_{TMAl} of 0, (b) ρ_{TMAl} of 0.25, and (c) ρ_{TMAl} of 0.50. For ρ_{TMAl} of 0, a dense array of InAs NWs is observed. Introduction of Al results in a dramatic change in NW morphology, number density, and directionality. Unlike the case of InGaAs NWs on SLG [4], we find that reduction in In-content, associated with incorporation of higher Al-content, does not induce NW bending.

Fig. 5 quantifies the length and diameter of InAlAs NWs grown at T_G = 600 °C under ρ_{TMAl} values between 0 and 0.5; data points represent mean values measured from >20 NWs. Compared to binary InAs NWs (i.e., $\rho_{TMAl} = 0$) grown at the same temperature, the introduction of TMAl causes a dramatic reduction of NW length and enhancement of NW diameter. This can likely be attributed to limited surface migration of Al atoms during epitaxy. Tapered NW morphologies are only observed under high ρ_{TMAl} conditions and at T_G = 600 °C, also likely due to low Al surface migration compared to In. Moreover, NW verticality suffers with increasing Al-content, such that mostly tilted NWs are found at ρ_{TMAl} = 0.5.

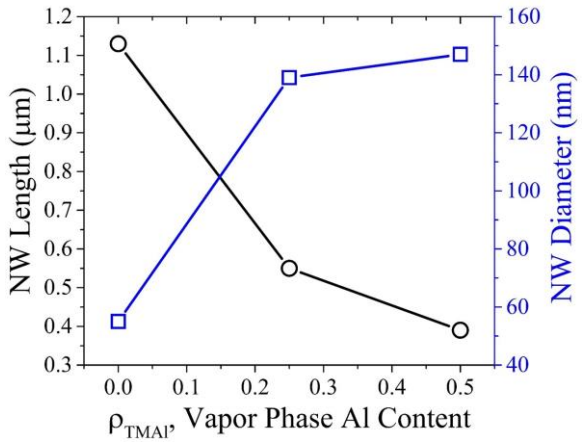

Fig. 5. Mean $In_xAl_{1-x}As$ NW length (black data points) and diameter (blue data points) vs. ρ_{TMAl} at T_G = 600 °C.

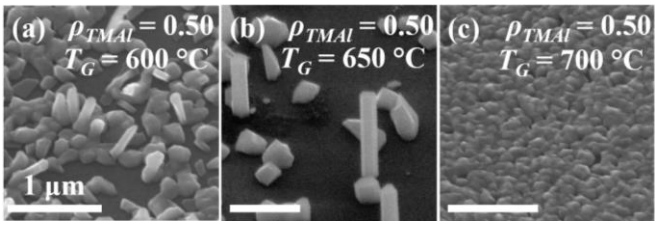

Fig. 6. 45º tilted-view SEM images of as-grown $In_xAl_{1-x}As$ NWs on SLG at T_G of (a) 600°C, (b) 650°C and (c) 700 °C. All scale bars represent 1 µm.

A growth temperature dependence study is performed for InAlAs NWs grown at constant V/III = 25 and ρ_{TMAl} = 0.50. Shown in Fig. 6 are 45° tilted-view SEM images of InAlAs NWs formed on SLG at T_G of (a) 600°C, (b) 650°C and (c) 700 °C. Growth at T_G = 600°C results in formation of very few vertically oriented NWs on SLG and favors formation of parasitic islands, from which NW structures may extend. However, a 50 °C increase in T_G modifies the growth kinetics such that the density of vertically-oriented NWs increases, while areal coverage of parasitic islands reduces. As T_G is raised further from 650°C to 700 °C, growth of InAlAs NWs is quenched, leading to formation of a contiguous III-V film.

This trend can be explained in terms of a balance between decomposition efficiencies of TMIn and TMAl and temperature-dependent surface mobility of In and Al atoms at these temperatures. Since TMIn shows near-unity decomposition efficiency in this T_G range [12], the change in surface diffusion and availability of Al atoms (i.e., decomposition percentage of TMAl) plays the predominant role. Thus, the abundance of available In atoms is less sensitive to T_G in the explored temperature range than the abundance of Al atoms, while In atoms experience enhanced surface migration compared to Al atoms at all temperatures [13, 14]. As a result, the limiting factor at 600 °C is likely the low thermally-promoted surface diffusion of both group-III species, leading to high polycrystalline island growth. Instead, at 700 °C, the limiting factor for surface diffusion is the abundance of Al atoms due to greater TMAl decomposition. This influence quenches NW growth and forces lateral extension of a high-density collection of polycrystalline islands, thereby leading to film formation. At intermediate temperatures, a balance point is reached between these competing factors. Thus, T_G = 650 °C may likely represent a tradeoff temperature at which sufficient thermally-promoted surface migration of less abundant Al atoms occurs, such that both group-III species can reach the top facets of <111> oriented nuclei and, consequently, accommodate vertical InAlAs NW formation.

As a final point of discussion, the results of vdWE for InAsP and InAlAs NW groups are compared. As briefly noted in the Introduction, due to the absence of covalent bond formation, strain sharing is inhibited at the III-V epilayer/graphene interface. Thus, the III-V lattice formed in the vdWE mode may not pseudomorphically adopt a lattice constant other than its inherent one. Additionally, for In-based structures grown in the vdWE regime on SLG, it has been shown that the lower-most flatly reconstructed III-V monolayer possesses a polar orientation such that group-III species are directly interfaced

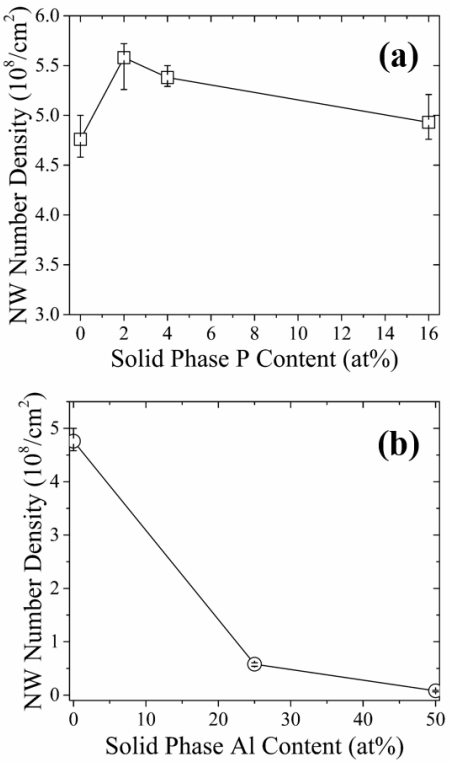

Fig. 7. (a) $InAs_yP_{1-y}$ NW number density versus percentage of solid phase P-content, (b) $In_xAl_{1-x}As$ NW number density versus percentage of solid phase Al-content.

with C [15]. In the case of InAs on SLG, the native InAs lattice allows for residence of In atoms above graphene H-sites; the same may also be expected for $InAs_{0.8}P_{0.2}$ [6]. While B-site residence is most energetically stable for both As and P atoms according to calculations by Nakada and Ishii [8], the residency competition between group-V species in the case of InAsP is not expected to change the position of In atoms from H-site to B-site. Therefore, formation of ternary $InAs_{0.8}P_{0.2}$ (i.e., in comparison to binary InAs) is not expected to shift In atom positions to B-sites. Correspondingly, little variation in the number density of NWs is observed comparing vdWE of InAs and InAsP on SLG. Fig. 7(a) quantifies the change in NW number density for $InAs_yP_{1-y}$ NWs grown under otherwise constant growth conditions while ρ_{PH_3} is varied between 0 and 0.98 (i.e., $1 \leq y \leq 0.84$). However, introducing Al as a group-III species, which can reside at the interface, into the InAs lattice significantly changes NW morphology and number density. As shown in Fig. 7(b), a ~60-fold reduction in NW number density results by increasing ρ_{TMAl} from 0 to 0.50. Chan et al. reported calculations of binding energy for various group-III metallic atoms on graphene [7]. For $In_xAl_{1-x}As$ with low Al content, both In and Al adatoms were shown to reside on the energetically favorable H-site [7, 8]. However, by increasing Al-content, a reduction in the $In_xAl_{1-x}As$ lattice constant forces an altered atomic configuration at the growth interface such that Al resides on the B-site [7, 8]. Since Al has a higher binding energy when situated above the B-site, formation of InAlAs NW structures (i.e., versus polycrystalline islands) on SLG likely becomes less favorable and NW growth becomes quenched (i.e., Fig 4).

IV. Conclusions

Formation of InAsP, InAlAs, and InP/InAsP NWs via pseudo-vdWE on SLG is reported for the first time. Self-assembly of $InAs_yP_{1-y}$ NWs on SLG is achieved for $1 \leq y \leq 0.8$. Solid phase P-content and number density of NWs are strongly dependent on growth temperature. Higher P-content NWs have been realized via a two-temperature growth regime. The dependence of $In_xAl_{1-x}As$ NW composition and morphology on growth temperature and ρ_{TMAl} have been investigated for $1 \leq x \leq 0.5$. Although NW number density was shown to have an inverse dependence upon Al-content, well-defined vertical NWs were realized at T_G = 650 °C and ρ_{TMAl} = 0.5. A general trend for vdWE of InAsP and InAlAs NWs has been discussed to relate NW number densities to lattice coordination and binding energy of growth species on SLG. We anticipate the use of such hybrid nanosystems in low-cost optoelectronics and high-efficiency tandem-junction photovoltaics.

Acknowledgment

This work is supported by the NSF under Award No. 1665086. M.A.S. wishes to acknowledge support from ICPRF program.

References

[1] G. Fiori *et al.*, "Electronics based on two-dimensional materials," *Nat. Nanotech.*, vol. 9, no. 10, pp. 768–779, Oct. 2014.
[2] Z. Liu, S. P. Lau, and F. Yan, "Functionalized graphene and other two-dimensional materials for photovoltaic devices: device design and processing," *Chem. Soc. Rev.*, vol. 44, no. 15, pp. 5638–5679, Jul. 2015.
[3] M. A. Baboli *et al.*, "Growth Parameter Space Mapping and Optimization of Self-Assembled InAs Nanowire Arrays on Graphene," (Submitted)
[4] P. K. Mohseni *et al.*, "$In_xGa_{1-x}As$ Nanowire Growth on Graphene: van der Waals Epitaxy Induced Phase Segregation," *Nano Lett.*, vol. 13, no. 3, pp. 1153–1161, Mar. 2013.
[5] E. A. Anyebe *et al.*, "Realization of Vertically Aligned, Ultrahigh Aspect Ratio InAsSb Nanowires on Graphite," *Nano Lett.*, vol. 15, no. 7, pp. 4348–4355, Jul. 2015.
[6] A. M. Munshi *et al.*, "Vertically Aligned GaAs Nanowires on Graphite and Few-Layer Graphene: Generic Model and Epitaxial Growth," *Nano Lett.*, vol. 12, no. 9, pp. 4570–4576, Sep. 2012.
[7] K. T. Chan, J. B. Neaton, and M. L. Cohen, "First-principles study of metal adatom adsorption on graphene," *Phys. Rev. B*, vol. 77, no. 23, p. 235430, Jun. 2008.
[8] K. Nakada and A. Ishii, "Migration of adatom adsorption on graphene using DFT calculation," *Solid State Commun.*, vol. 151, no. 1, pp. 13–16, Jan. 2011.
[9] J. Wallentin, D. Kriegner, J. Stangl, and M. T. Borgström, "Au-Seeded Growth of Vertical and in-Plane III–V Nanowires on Graphite Substrates," *Nano Lett.*, vol. 14, no. 4, pp. 1707–1713, Apr. 2014.
[10] Y. J. Hong, W. H. Lee, Y. Wu, R. S. Ruoff, and T. Fukui, "van der Waals Epitaxy of InAs Nanowires Vertically Aligned on Single-Layer Graphene," *Nano Lett.*, vol. 12, no. 3, pp. 1431–1436, Mar. 2012.
[11] G. B. Stringfellow, *Organometallic Vapor-Phase Epitaxy: Theory and Practice*. Elsevier, 1999.
[12] N. I. Buchan, C. A. Larsen, and G. B. Stringfellow, "Mass spectrometric studies of trimethylindium pyrolysis," *J. Cryst. Growth*, vol. 92, no. 3, pp. 591–604, Oct. 1988.
[13] D. W. Squire, C. S. Dulcey, and M. C. Lin, "Mechanistic studies of the decomposition of trimethylaluminum on heated surfaces," *J. Vac. Sci. Technol., B*, vol. 3, no. 5, pp. 1513–1519, Sep. 1985.
[14] C. Agert, P. Lanyi, and A. W. Bett, "MOVPE of GaSb, (AlGa)Sb and (AlGa)(AsSb) in a multiwafer planetary reactor," *J. Cryst. Growth*, vol. 225, no. 2, pp. 426–430, May 2001.
[15] Y. J. Hong, J. W. Yang, W. H. Lee, R. S. Ruoff, K. S. Kim, and T. Fukui, "Van der Waals Epitaxial Double Heterostructure: InAs/Single-Layer Graphene/InAs," *Adv. Mater.*, vol. 25, no. 47, pp. 6847–6853.